5250–5261 *Nucleic Acids Research, 2005, Vol. 33, No. 16*
doi:10.1093/nar/gki822

RNase III cleavage demonstrates a long range RNA: RNA duplex element flanking the hepatitis C virus internal ribosome entry site

Nerea Beguiristain[1], Hugh D. Robertson[2] and Jordi Gómez[1,3,*]

[1]Laboratorio de Medicina Interna, Hospital Vall d'Hebron, Barcelona 08035, Spain,
[2]Department of Biochemistry, Weill Medical College of Cornell University, New York, NY 1002, USA
and [3]Centro Investigación en Sanidad Animal INIA, Valdeolmos, Spain

Received May 3, 2005; Revised July 22, 2005; Accepted August 23, 2005

ABSTRACT

Here, we show that *Escherichia coli* Ribonuclease III cleaves specifically the RNA genome of hepatitis C virus (HCV) within the first 570 nt with similar efficiency within two sequences which are ~400 bases apart in the linear HCV map. Demonstrations include determination of the specificity of the cleavage sites at positions C^{27} and U^{33} in the first (5′) motif and G^{439} in the second (3′) motif, complete competition inhibition of 5′ and 3′ HCV RNA cleavages by added double-stranded RNA in a 1:6 to 1:8 weight ratio, respectively, 50% reverse competition inhibition of the RNase III T7 R1.1 mRNA substrate cleavage by HCV RNA at 1:1 molar ratio, and determination of the 5′ phosphate and 3′ hydroxyl end groups of the newly generated termini after cleavage. By comparing the activity and specificity of the commercial RNase III enzyme, used in this study, with the natural *E.coli* RNase III enzyme, on the natural bacteriophage T7 R1.1 mRNA substrate, we demonstrated that the HCV cuts fall into the category of specific, secondary RNase III cleavages. This reaction identifies regions of unusual RNA structure, and we further showed that blocking or deletion of one of the two RNase III-sensitive sequence motifs impeded cleavage at the other, providing direct evidence that both sequence motifs, besides being far apart in the linear RNA sequence, occur in a single RNA structural motif, which encloses the HCV internal ribosome entry site in a large RNA loop.

INTRODUCTION

The hepatitis C virus (HCV) is a human pathogen causing chronic liver disease in 170 million people worldwide (1). The virus is classified within the family *flaviviridae* (1). The RNA genome begins with a 5′-untranslated region (5′-UTR) that extends from position 1 to the AUG at position 342, continues in the core (C) coding region which is the first coding locus of a long open reading frame and ends in a 3′ non-coding region (1). The secondary structure of the 5′-UTR of HCV has been extensively studied since the early nineties (2,3). Biochemical and functional studies revealed that the HCV 5′-UTR folds into a highly ordered complex structure with multiple stem loops (2–4) containing two distinct RNA elements, a short 5′-proximal RNA element (nucleotides 1–43) that regulates HCV replication and translation (5–7) (domain I) and a longer internal ribosome entry site (IRES) element, including nucleotides 44–370 and forming domains II, III and IV. Mutational analysis has revealed that maintenance of the IRES structural domains is critical for cap-independent initiation of translation of the viral polyprotein (8–11).

Comparison of HCV 5′-UTR sequences from different HCV genotypes has revealed that variation is very limited to particular sites (12). The sites of genotype variability are usually covariant substitution sites and they maintain the base paring required for the 5′-UTR secondary structure model (13,14). There is an interesting exception reported by Honda *et al*. (15) in an apparently unpaired region, between positions 21 and 43 where bases A^{34} G^{35} in genotype 1b correspond to G^{34} A^{35} in genotype 1a. The presence of A^{34} G^{35} has been associated with a 2-fold decrease of the translational efficiency in genotype 1b. This difference was only observed when the translated fragment contained the region downstream the

*To whom correspondence should be addressed. Tel: +34 916202300 ext. 125; Fax: +34 916202247; Email: jgomez@vhebron.net, castilla@inia.es

AUG codon, supporting the idea of a long distance RNA–RNA interaction between the region containing the AG dinucleotide preceding the IRES and the capsid coding region (15). Subsequently, it was observed that mutations introduced to decrease hypothetical Watson–Crick base pairing between bases 24–38 and 428–442 could affect levels of IRES-mediated translation, and that compensatory mutations in this complementary motif re-established normal levels of translation directed by HCV IRES (16). Kim *et al*. proposed a hypothetical double-stranded RNA (dsRNA) motif whose duplex stability could regulate IRES activity. Nevertheless, direct structural proof for these kinds of proposals, derived from the evolutionary and sequence correlations, is lacking.

RNase III was discovered in 1967 as the third RNase activity of *Escherichia coli* (17,18). It was defined as a specific dsRNase that cleaved regions of 20 or more base pairs of RNA–RNA duplex structure and shown to participate in several RNA processes, including maturation of rRNA (19,20). RNase III may also cleave certain other specific regions with less perfect base pairings, which invariably contain approximately two turns of more or less regular dsRNA and additional sequence or structural elements which determine the way these substrates are cleaved (20). A well-studied example is the processing of the early mRNA region of the bacteriophage T7 (21). A set of specific cleavage reactions carried by *E.coli* RNase III enzyme which are favored at high enzyme:substrate ratios and at lower, rather than higher, monovalent cation concentration was discovered in 1976 (21). These were referred to as secondary cleavages; they behave like primary cleavages in the following way: they are effectively inhibited by dsRNA competitors for RNase III primary cuts; they are not inhibited by large molar excess of ssRNA and they are reproducible and specific, yielding 5′ phosphates and 3′ hydroxyls (21). In two well-characterized RNase III substrates, the T7 1.1mRNA (22) (between genes 1.0 and 1.1 of T7 early region) and a region next to T7 1.2 mRNA (23), primary and secondary cleavages occur in the opposite side of a hairpin loop ~20 bp long, in a central region where the base pairing is less regular. Some secondary cleavages, such as that of R1.2 T7 mRNA, take place *in vivo*, although only 40% of the time (24).

Here, we found that two linked RNase III secondary cleavage sites flank the HCV IRES of genotype 1b. We also report that the two cleavages are specific to *E.coli* RNase III and show where the cleavages occur and the category into which they fall. Special caution was exercised because of using a commercial RNase III preparation that arises from cleavage of fusion proteins, to ensure that HCV cleavages are not the result of accompanying RNases or an artificial broadening of RNase III specificity. Finally, we report that the sequences carrying both cleavage sites interact to construct a single RNase III signal. This provides a direct proof for the presence of a structural motif with dsRNA characteristics between a region immediately preceding the IRES around positions C^{27} and U^{33} and a complementary downstream sequence surrounding positions G^{439}.

Taken together, the sensitivity of HCV RNA to RNase III described here represents the structural correlate of previous functional studies (16) and evolutionary observations (15) that allow us to conclude that the HCV IRES is embedded in a larger RNA structure.

MATERIALS AND METHODS

RNase III enzyme

RNase III enzymes were obtained from commercial or natural sources (18). Commercial Ambion enzyme was the one used for most of the experiments related to HCV RNA structure. Commercial enzymes from New England Biolabs and Epicenter were used as indicated in Results. Natural RNase III enzyme was obtained from a phosphocellulose column peak or from a DEAE–Sephadex column peak and was used to evaluate the specificity of the commercial Ambion enzyme under our reaction conditions.

RNA transcripts

The DNA templates for HCV RNA transcripts were derived from the plasmid vector pN (1–4728) Bluescript, which contains nt 1–4728 of HCV under the T7 promoter. All RNA transcripts include the first base of the HCV genome and end at positions 402 (Aat-II) S_3, 466 (PCR product) S_2 and 570 (Blp-I) S_1. The PCR product ending at base 466 was generated by amplification of pN (1–4728) with upstream primer (5′-CGCGGATCCTAATACGACTCACTATAGGC-CGCCCCGATTGGGGGCGA-3′ (which serves to introduce the T7 promoter in the PCR product) and a downstream primer (5′-GGGCCCCTGCGCGGCAACAG-3′). The T7 R1.1 RNA transcript used is a truncated version of the one described before (25). The RNA product is 60 nt long and contains the bacteriophage T7 'R1.1' primary and secondary cleavage sites.

In vitro transcription

To obtain the internally labeled substrates for cleavage assays, 1–2 μg of DNA template were transcribed *in vitro* (1 h at 37°C) with [α-^{32}P]GTP followed by a 5 min treatment with RNase-free DNase I at 37°C. Cellulose CF11 chromatography was used to eliminate DNA fragments and non-incorporated nucleotides. Transcripts were then purified by gel electrophoresis under denaturing conditions on 4% polyacrylamide gels containing 7 M urea. Bands were visualized by autoradiography, excised from the gel and eluted in buffer 100 mM Tris–HCl, pH 7.5 and 10 mM EDTA, pH 7.5. The concentration of radioactive transcripts was determined by calculating the amount of incorporated [α-^{32}P]GTP based on scintillation counting (26).

'Low specific activity' labeled RNA transcripts were made by scaling up by 40-fold the transcription reaction described above, and with 1/100 of the concentration of the radioactive nucleotide.

Obtaining of 5′ end-labeled and 3′ end-labeled transcripts

Unlabeled 'cold' transcripts prepared in standard transcription reactions without added radioactive nucleotide label were subsequently reacted as follows.

3′ End labeling. Aliquots containing 40 U T4 RNA ligase and a molar ratio of 2:1 pmol of 5′ [^{32}P]pCp with respect to RNA were mixed. The reaction was carried out in 30 μl of 50 mM Tris–HCl, pH 7.5, 10 mM $MgCl_2$, 10 mM DTT, 1 mM ATP, 0.01% BSA and 10% dimethyl sulfoxide, RNasin (20 units) and T4 RNA ligase (40 units). The reaction mixture was

incubated 4 days at 4°C. The labeled RNA was purified again using the electrophoretic procedure described above.

5′ End labeling. Reactions were carried out using [α-^{32}P]GTP and the enzyme guanylyl transferase, and followed the same purification procedure. First, 8 µl of [α-^{32}P]GTP were dried in a Speedvac. Meanwhile, the reaction mixture (20 µl) contained 50 mM Tris–HCl, pH 8.0, 6 mM KCl, 1.2 mM Mg Cl_2, 1 U RNasin, 50 nM *S*-Adenosyl–Methionine (Sigma) and 10 nM DTT was prepared. Finally, the 'cold' RNA transcript is added to a 2.5 µM final concentration. This capping reaction was initiated by the addition of 1 µl guanylyl transferase (recombinant enzyme provided by J. Martinez) and incubated at 37°C for 4 h. The reaction was stopped by the addition of 2 vol of loading buffer (0.3% Bromophenol Blue, 0.3% Xilene-cianol, 10 mM EDTA pH, 7.5 and 97.5% desionized formamide) and the transcript was purified by denaturing polyacrylamide gel electrophoresis using the procedure described above.

RNase III cleavage assay: standard and working conditions

Standard RNase III conditions include a buffer containing 0.01 M Tris–HCl, pH 7.6, 0.13 M NH_4Cl and 0.01 M $MgCl_2$. The salt and buffer conditions used for all of our initial experiments on HCV RNA cleavage by RNase III were the same used previously to detect RNase P cleavage of a tRNA-like structure near the AUG start triplet in the HCV IRES. These are not standard RNase III conditions and are referred in the text as 'working conditions'. HCV RNA substrate (0.6 nM final concentration) was pre-heated at 90°C for 1 min, before the addition of reaction buffer [10 mM HEPES–KOH, pH 7.5, 10 mM $Mg(OAc)_2$ and 100 mM $NH_4(OAc)$] and left to cool down to room temperature. Cleavage reactions were performed with 20 U RNAsin, and 0.0005 U/µl (final concentration) of *E.coli* RNase III (Ambion), in the presence of 1 µg/µl of yeast tRNA, and were carried out at 37°C in a volume of 10 µl for 1 h. These optimal conditions were used in all of the experiments. Cleavage products were separated on denaturing polyacrylamide gels and visualized by autoradiography.

Quantitative data relating to RNase III cleavage kinetics were obtained using a Radioisotopic Image Analyser BAS-1800 (Fuji film). The percentage of uncleaved material was calculated as the ratio of uncleaved material/starting material.

RNA sequencing with partial nuclease digestion

Partial RNase T1 digestion assays on 5′ labeled transcripts. Aliquots containing 2×10^4 Cerenkov c.p.m. of the Cap-5′-Labeled RNA transcripts were mixed with 2.5 µg carrier tRNA in 1 mM Tris–HCl (pH 7.5) and 1 mM EDTA (final concentration). Cleavage reactions were initiated by the addition of 0.1 µg RNase T1 and incubated at 37°C for 20 min in a final reaction volume of 10 µl.

Nuclease P1 assays on end-labeled transcripts. For RNase reactions, the digestion mixture (10 µl) contained $\sim 2 \times 10^4$ Cerenkov c.p.m. of the 5′ or 3′ end-labeled transcript and 2.5 µg of carrier tRNA in 40 mM NH_4OAc (pH 5.3), 0.4 mM $ZnS0_4$ during 5 min at 70°C. Cleavage reactions were initiated by the addition of 0.001 µg/µl nuclease P1 (Calbiochem) and incubated at 70°C for 1 min (27).

Alkaline hydrolysis reactions. Aliquots containing 10^4 Cerenkov c.p.m. of end-labeled RNA were incubated with 2 µg of carrier tRNA in 0.2 M $NaHCO_3$–Na_2CO_3 (pH 9) and 1 mM EDTA for 5 min at 90°C (27).

All reactions were stopped with 1 vol of loading buffer and maintained in dry ice until loading in 4% polyacrylamide–urea sequencing gel.

Circularization assay

The pre-labeled P2 was incubated with T4 RNA ligase using the same conditions described above (see 3′ end-labeled transcript), and the reaction was carried out in 10 µl final volume. In a later step, this reaction was treated with 2.5 µg tRNA, 30 mM EDTA, 3% SDS and 0.5 mg proteinase K (previously pre-heated at 65°C for 1 min) at 65°C for 5 min. After phenol treatment and precipitation with acetate and ethanol, the results were visualized on 4% denaturing polyacrylamide gel.

Polynucleotide kinase labeling

The product bands purified by preparative gel electrophoresis were labeled using the Kinase Max Kit (Ambion).

Competitive reactions

Competitive inhibition. The experiments consisted of incubating the same amount of end-labeled HCV transcript with increasing concentrations of dsRNA (of substantial length, from a virus grown in *Penicillium chrysogenum*) from 2- to 12-fold to inhibit the HCV RNA cleavages. The conditions for assaying RNase III cleavage are described above. Poly(I–C) (Sigma) was used for other reactions.

Reverse competitions. The internally labeled transcript R1.1 is incubated with increasing concentrations (from 1/4- to 4-fold) of cold HCV RNA in the same conditions described above.

RNA fingerprinting

Oligonucleotides created by RNase T1 digestion of [α-^{32}P]GTP labeled R1.1 RNA were fractionated to yield 2D fingerprints [first dimension by electrophoresis and second by homocromatography exactly as described previously (28)].

RESULTS

Cleavage of HCV RNA transcripts

Figure 1 is a schematic drawing of the HCV genome, above which appear the S_1, S_2 and S_3 transcripts located at the 5′-UTR and the first one-third of the Core coding region, all starting at position 1 of the HCV genome. The substrates are consecutively shortened at their 3′ ends (position 570 in S_1, 466 in S_2 and 402 in S_3). Initial *E.coli* RNase III experiments involved the S_1 substrate transcript, either internally labeled (Figure 2A), 'cap' labeled (Figure 2B) or labeled at its 3′ end (Figure 2C) subsequent experiments utilized the shorter S_2 transcript, labeled in the same way (data not shown), allowing us to distinguish between S_1 partial cleavage products P1–P2 and P2–P3 or complete digestion products P1, P2 and P3, and to position the cleavage sites in the S_1 570-base fragment,

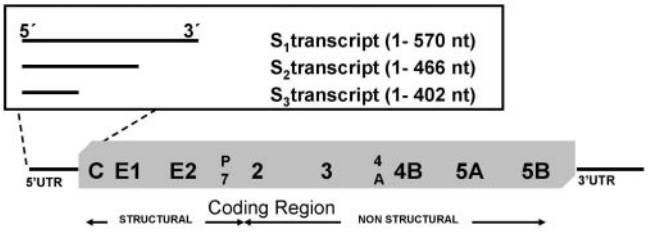

Figure 1. Organization of the HCV genome and localization of HCV transcripts in the viral genome. Relative location of the 5′-UTR structural genes (C, Core; E1 and E2, envelope genes 1 and 2), the p7 coding region and non-structural genes (NS2 to NS5) and the 3′-UTR. S_1 (1–570), S_2 (1–466), S_3 (1–402) have been used as substrates in the *E.coli* RNase III assays. All transcripts initiate at the first base of the HCV genome, contain the complete 5′ UTR and expand to different sites within the Core-coding region.

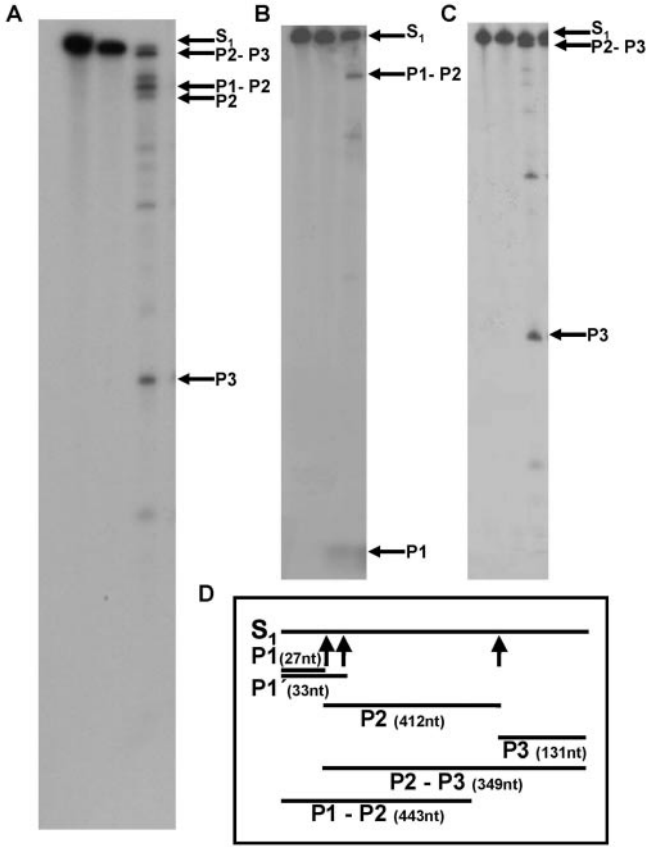

Figure 2. Localization of RNase III cleavage sites on HCV transcripts in the viral genome. (**A**–**C**) Autoradiograms of *E.coli* RNase III cleavage of internally labeled, 5′ end-labeled and 3′ end-labeled S_1 transcripts, respectively. Lane 1, the transcript alone incubated on ice; lane 2, transcript incubated in under 'working conditions'; lane 3, RNase III cleavage reaction. The arrows indicate the substrate band (S_1) and the product bands–partial products (P1–P2) and (P2–P3) and total products (P1, P2 and P3). (**D**) Diagram of the cleavage sites of HCV RNA by *E.coli* RNase III. S_1 transcript (1–570) is represented with a line. RNase III cleavage sites in the positions 27, 33 and 439 respectively, are indicated by three arrows. Below are represented the final and partial cleavage products bands observed on a 4% polyacrylamide electrophoresis gels, (P1, P1′, P2 and P3) and (P1–P2, P2–P3), respectively.

as shown in Figure 2D. Additional bands that may be seen in the gel, which are not explored in the present work, are dependent on higher RNase III concentration and may correspond to less sensitive sites for RNase III.

RNase III is responsible for the HCV RNA cuts

The key experimental question of the HCV RNA cleavages obtained in the reactions involving commercial RNase III is whether the cleavages are performed by RNase III itself, rather than by a co-purified contaminant activity. The commercial RNase III used in this study arises by cleavage of fusion protein and is purified through various steps with a focus on dsRNA cleavage, rather than the processing of long ssRNA with a few specific sites for cleavage. This leaves open the possibility of contamination by traces of conventional RNases, which can cleave ssRNA, or that the recombinant enzyme had acquired a subtly broadened specificity. In order to determine the specificity of HCV cleavages by RNase III in this work, two series of experiments were performed: one on the HCV RNA–RNase III reaction and its cleavage products (classified as direct and indirect methods, respectively); the other comparing the action of commercial RNase III preparations and natural *E.coli* RNase III enzyme purified by standard techniques (18,21) on the well-known RNAse III substrate, bacteriophage T7 R1.1 mRNA.

Direct method: end group determination and cleavage precision by RNA sequencing

Specific cleavage positions. If RNase III is responsible for HCV RNA cleavage and if it were to cleave HCV RNA with the same specificity as it does other substrates, the site of cleavage should be between precise nucleotide positions (23,25,29,30).

Cleavage site within the first (5′) domain. Non-radioactive (cold) S_1 was 5′ end-labeled with [α-^{32}P]GTP in the presence of guanylyl transferase and purified by gel electrophoresis. A fraction of the labeled RNA was incubated with *E.coli* RNase III and another fraction was subjected to partial digestion with nuclease P1, or to partial hydrolysis with alkali (OH^-). RNase III products and partial P1 and OH^- products were run in parallel on 20% acrylamide gels. Two product bands appeared in close proximity in the RNase III lane (Figure 3A, lane 2). In relation to the mobility of the OH^- and P1 partial products (Figure 3, lanes 3 and 4, respectively), and counting from the first band, it was possible to conclude that RNase III is cleaving the phosphosdiester bond of a percentage of S_1 molecules between bases C^{27} and C^{28} and the rest between bases U^{33} and A^{34}. The percentage of molecules cleaved at one or the other position varied between different cleavage reactions, probably because of small experimental variation (data not shown).

Cleavage site within the second (3′) domain. Because the RNase III cleavage site in the second (3′) domain was apparently too far from the S_1 3′ end to discriminate its exact position in a sequencing gel, we prepared a shortened transcript at its 3′ end, S_2 (see Figure 1). Cold S_2 transcript was 3′ end labeled with [α-^{32}P]pCp and T4 RNA ligase. The downstream RNase III cleavage product of S_2 was named P3* since it is a shortened version of product P3. P3* was gel purified and subjected to partial digestion with T1 RNase and hydrolysis with OH^-. The electrophoretic mobility of P3* corresponds to a fragment with two additional bases (counting from the 3′ end of P3*) than the partial fragment generated by the T1 after cleaving at position G^{441} (see Figure 3B legend and the list of the T1-resistant oligonucleotides of P3*, Figure 3C and D).

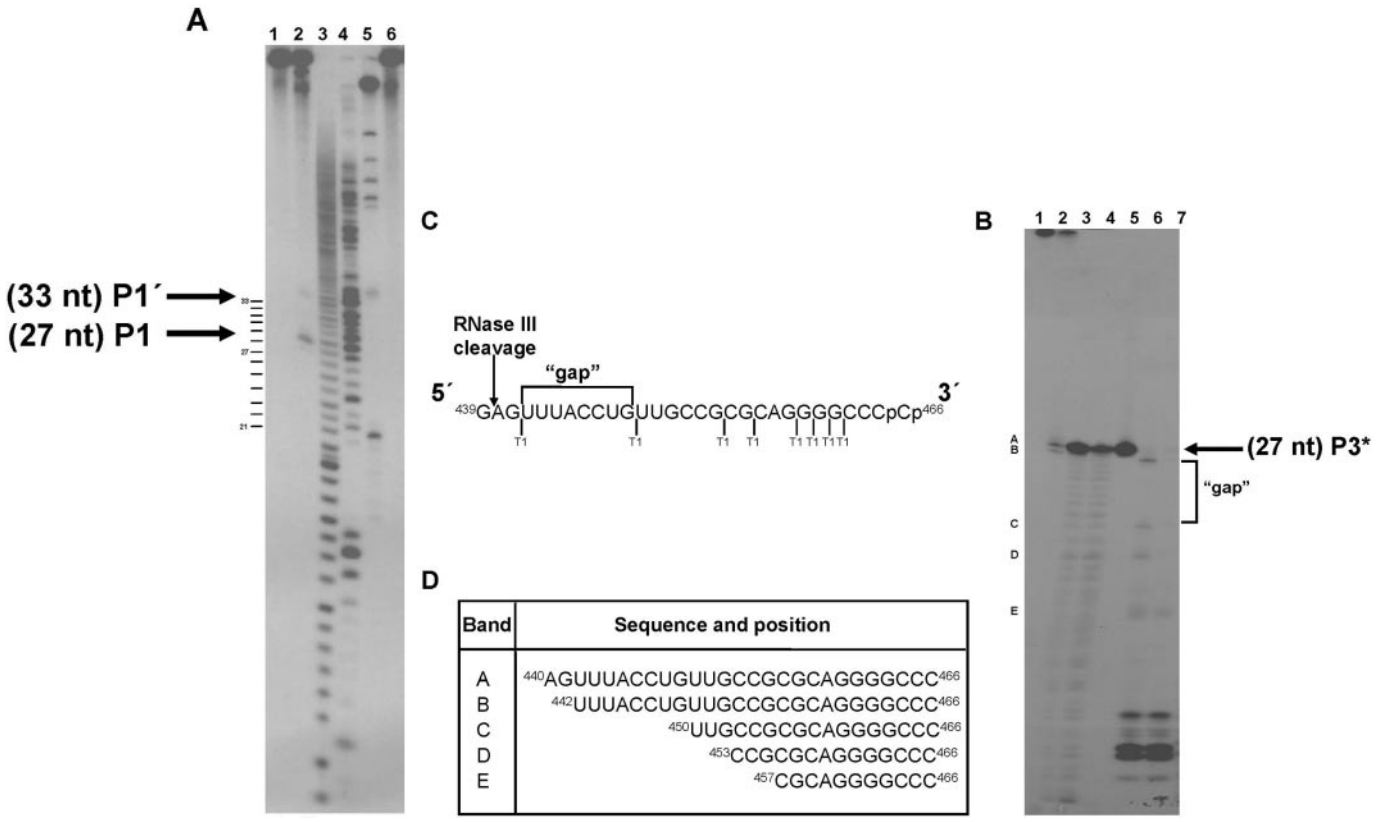

Figure 3. Determination of the cleavage sites in the HCV transcript. (**A**) To determine the cleavage sites near the 5′ end, a 'Cap' labeled S_1 was prepared. Lane 1, S_1 RNA transcript alone incubated on ice; lane 2, S_1 incubated with RNase III (see conditions in Figure 2). Arrows indicate the most prominent bands (P1, P1′); lane 3, alkaline hydrolysis reaction; lane 4, S_1 RNase P1 reaction; lane 5, RNA molecular weight markers composed of transcripts with a length of 21, 40, 69, 76, 77, 109 and 135 nt; lane 6, S_1 incubated under 'working' conditions buffer without enzyme. Samples were electrophoresed on a 20% denaturing polyacrylamide gel. The RNase III cleavage products (with expected 3′ OH end groups) run between two alkaline hydrolysis products (mixtures of RNA fragments with 3′P and 2′P end groups), and have been numbered according to the band running faster. Further experiments based on fingerprinting of internally labeled RNA are in progress to confirm the cleavage position presented here. (**B**) For determination of the cleavage site near the 3′ end, the S_2 (1–465) transcript was labeled with ^{32}pCp at its 3′ end with the T4 RNA ligase, cleaved with RNase III, and the most 3′-proximal product P3* (indicated by an arrow) gel purified on a 20% denaturing polyacrylamide gel. Lane 1, S_2 transcript on ice; lane 2, S_2 treated with RNase III (standard conditions); lane 3 and 4, partial hydrolysis of P3* with OH^- after incubations of 4 and 8 min, respectively; lane 5, P3* alone; lanes 6 and 7, partial digestions with nuclease T1 at 0.01 and 0.02 μg/μl final concentrations, respectively. The product bands of RNase T1 identified as A, B, C, D, E, at the left of the electrophoresis gel are described in (**D**). (**C**) Representation of the 3′ end RNA sequence of S_2 containing the P3* fragment. RNase T1 cleavages after every G-residue are marked. A gap of 8 nt between the B and C product bands in the gel could be clearly positioned between positions U^{442} and G^{450}, the largest RNase T1 digestion product of the P3* fragment. This gap serves as a reference to localize the cleavage site two positions upstream, between bases G^{439} and A^{440}.

This result located the distal RNase III cleavage between bases G^{439} and A^{440}.

E.coli RNAse III cleaves perfect dsRNA sequences of low complexity and many other substrates leaving 2 nt overhands products. The pattern of cleavage of the duplex at sites 27/439 differs from the general pattern of cleavage of a regular dsRNA at a given target site. Nevertheless, in cases where secondary RNAse III cleavage sites have been mapped, as in the R1.1 and R1.3 T7 RNA substrates, cleavages may produce a variety of extremes.

Biochemical characterization. One of the distinctive properties of RNase III is that it releases cleavage products containing 5′ PO_4 and 3′OH end groups (23,31). Contaminating RNases almost invariably cleave to yield 5′ hydroxyl and 2′, 3′ phosphate end groups, and very few RNases cleave the phosphodiester backbone through the same mechanism used by RNase III (32,33). To identify the end group of the reaction products we carried out two different kinds of experiments. One was an enzymatic approach; the other, based on electrophoretic mobility.

Enzymatic approach. T4 RNA ligase may add a [α-^{32}P]pCp nucleotide to the 3′ OH end of an RNA fragment, and also may circularize terminal RNA fragments ending with a 5′ P and a 3′ OH. On the other hand, T4 polynucleotide kinase can introduce a ^{32}P from [γ-^{32}P]ATP into the 5′ end of an RNA fragment only if that end already has a 5′ OH, or has been previously dephosphorylated by treatment with a phosphatase. From all total and partial cleavage products generated after RNase III cleavage of S_1, P2 has the two newly generated termini. Thus, efforts were first concentrated on the determination of the end groups of P2. Thus, S_1 was labeled at low specific radioactivity (enough to trace its electrophoretic mobility but low enough to permit an increase of incorporated radioactivity in the subsequent end-labeling reactions with the RNA ligase or polynucleotide kinase). Product band P2 was purified from other S_1 cleavage products after electrophoresis, and the recovered radioactivity was divided into

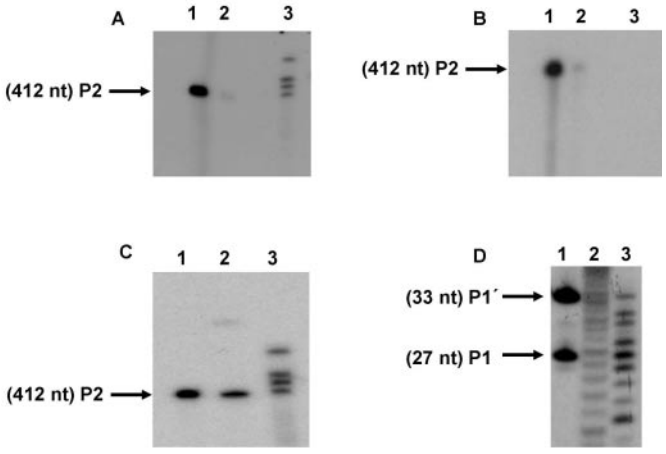

Figure 4. Biochemical characterization of HCV RNase III cleavage product end-groups. S_1 was internally labeled at low specific radioactivity and cleaved with RNase III. P2 purified from the gel was subjected to different specific enzymatic reactions to determine chemical groups of the (**A**): 3′ end. Lane 1, P2 labeled with [^{32}P]pCp and T4 RNA ligase; lane 2, P2 alone; lane 3, control bands resulting from a standard reaction of RNase III on S_1. (**B**) 5′ End. Lane 1, P2 central product band labeled with T4 polynucleotide kinase and [γ-^{32}P]ATP after treatment with alkaline phosphatase; lane 2, P2 was identically treated as before without prior incubation with alkaline phosphatase; lane 3, P2 untreated. (**C**) 3′ and 5′ ends by P2 product circularization: lane 1, P2 alone; lane 2, P2 circularization with T4 RNA ligase. The band that corresponds to circularized P_2 migrates more slowly than the starting material; lane3, standard RNase III reaction. (**D**) Coincident mobility of the 5′-terminal RNase III and nuclease P1 cleavage products of substrate S_1 5′ Cap labeled S_1 incubated with: lane 1, RNase III (the positions of the products P1 (27 nt) and P1′ (33 nt) are indicated by arrows); lane 2, OH^- hydrolysis; lane 3, nuclease P1 treatment.

three aliquots. The resulting RNA was proven to be (i) actively labeled at its 3′ end by T4 RNA ligase and [α-^{32}P]pCp, as shown by an increase in the label in the autoradiogram in the lane representing the starting material (Figure 4A, lane 2) as compared with that subsequently treated by the ligase (Figure 4B, lane 1), demonstrating a 3′ OH end; (ii) labeled in the 5′ end with T4 polynucleotide kinase and [γ-^{32}P]ATP preferentially when it was previously dephosphorylated by treatment with alkaline phosphatase enzyme (Figure 4B, lane 1) compared with when it was not (Figure 4B, lane 2), demonstrating the presence of a phosphate group in its 5′ end; (iii) circularized when incubated with T4 RNA ligase. In the electrophoresis autoradiogram (Figure 4C), it was possible to observe a more slowly migrating band (lane 2) in relation to untreated material (lane 1) that corresponds to circularized P2, proving in a single reaction the specific chemistry of RNase III reflected in both end groups at once.

The end-labeling or circularizing experiments described above were also performed on total and partial digestion fragments of S_1 (data not shown) proving the appropriate chemical groups: specifically, RNA ligase was able to label the 3′ end of P1, P2 and P1–P2. Dephosphorylation-dependent kinasing was demonstrated in P2 and P2–P3. Circularization was also demonstrated in P2–P3, but failed as expected in P1–P2, because of the presence of a 5′ pppG in P1 (pppG is not a substrate for RNA ligase).

Electrophoretic mobility. This second approach was based on the different electrophoretic motilities of RNA molecules depending on the nature of the chemical end group. Alkaline hydrolysis releases products with 5′ OH and a 2′–3′ cyclic phosphate ends, while nuclease P1 releases products with changed polarity: 5′ PO_4 and 3′ OH (27). Electrophoretic mobility of the products from P1 digestion labeled at their 5′ ends were compared, in sequencing gels, with the mobility of a product ladder generated by partial digestion of S_1 substrate with alkali or with P1 nuclease. The arrows on the left of Figure 4D indicate the position of the two 5′ S_1 products (see S_1 cleavage scheme in Figure 1); the mobility is parallel to P1 nuclease products (lane 3), in agreement with the hypothesis that RNase III cleavage has occurred, producing 5′ phosphate end groups. Only the end-groups of the shortest products of the RNase III treatment of HCV IRES substrates, P1 and P1*, could be tested in this kind of analysis, which is limited by the resolution of the sequencing gels.

Indirect methods: competitive and reverse competitive inhibition

Two additional strategies were used to demonstrate that RNase III, and not a contaminant in the enzyme preparation, was responsible for the processing reaction in S_1 and S_2 substrates. All competition reactions, direct and reverse, were performed in the presence of an excess high amount (2 μg) of unlabeled tRNA per reaction, which is a large excess over the competitor RNAs involved in the reaction, and eliminates the effects of non-specific inhibition by increasing the total amount of RNA in the reaction.

(i) *Competitive inhibition*. This experiment consisted of incubating the same amount of labeled HCV RNA S_1 with increasing concentrations of cold natural dsRNA (from 2- to 12-fold excess) to inhibit HCV RNA cleavages. 'Cap' labeled or 3′ end-labeled HCV S_1 RNAs were used, respectively, as appropriate to follow the P1 or P3 short product fragments in 14% and 20% polyacrylamide gels. As RNA competitor we employed a dsRNA of substantial length from a virus grown in *Penicillium chrysogenum* (PC RNA) which is a known substrate for *E.coli* RNase III (30,31). When this unlabeled (cold) dsRNA, from 20 to 120 ng, was included in the RNase III cleavage reactions of 'cap' labeled and 3′ labeled S_1, the amounts of HCV cleavage products were decreased with increased competitor concentration and reached total inhibition at a weight ratio of 1 to 6 PC RNA/HCV RNA for the 5′ end cleavage (Figure 5A, lane 6) and 1 to 8 for the 3′ end cleavage (Figure 5B, lane 7). Similar results were obtained using S_2 as a substrate for both sites (data not shown).

(ii) *Reverse competition*. In competition experiments reciprocal to those shown in Figure 5, we tested the ability of S1 to compete for RNase III activity with a 60-base RNA fragment of the natural substrate, phage T7 early precursor mRNA R1.1 (24,25). This fragment was internally labeled with [α^{32}P]GTP during transcription from a synthetic DNA template and was used as a substrate for the *in vitro* RNase III cleavage reactions that were competed by increasing concentrations of cold HCV S_1 RNA, from 0.45 to 7.2 nM. About 50% inhibition was reached at a concentration ratio of 1 HCV RNA/T7 R1.1 RNA (Figure 5C, lane 7). Reverse competition experiments were also performed with S_2 as RNA competitor and we obtained the same results (data not shown).

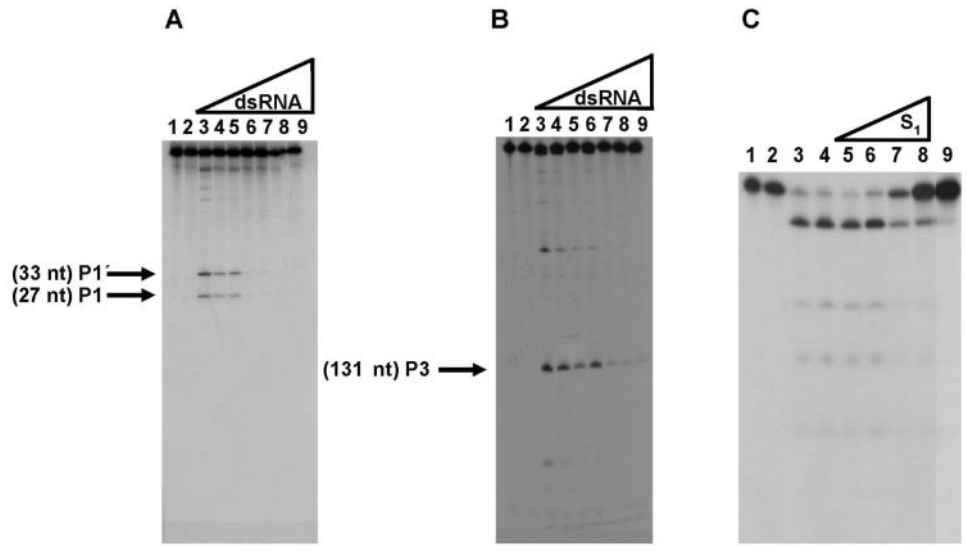

Figure 5. Competition assays. (A and B) dsRNA competes with and inhibits the RNase III-specific cleavage of HCV RNA. Cleavage by RNase III of S_1 transcript labeled at (**A**) 5′ end; (**B**) 3′ end, in the presence of increasing concentrations of competitor dsRNA. (A) Lanes 1 and 2 correspond to 5′ end-labeled RNA alone (incubated on ice) and incubated with buffer, respectively; lane 3, standard reaction with RNase III; lanes 2–9, cleavage reactions using a constant concentration of S_1 (10 ng) and increasing concentrations of dsRNA (20, 40, 60, 80, 100 and 120 ng, respectively). (B) Identical to (A) but using 3′ end-labeled S_1. (**C**) Reverse competition of RNase III cleavage of T7 R1.1 RNA with HCV RNA. A constant amount of a 60 nt fragment of T7 R1.1 RNA (internally labeled) was cleaved in the presence of increasing concentrations of HCV RNA S_1 without label. Lane 1 and 2, RNA T7 R1.1 alone or incubated with buffer, respectively; lane 3, standard RNase reaction, but with final concentration of RNase III of 0.0001 U/µl; lane 4, standard reaction with RNase III (0.0005 U/µl); lanes 5–9, RNase III cleavage of a constant concentration of T7 R1.1 RNA (1.8 nM) and increasing concentrations of S_1 RNA (0.45, 0.9, 1.8, 3.6 and 7.2 nM respectively); lane 9, inhibition of T7 R1.1 RNA cleavage with 300 ng of *Penicillium chrysogenum* dsRNA (positive control).

Characterizing the activity of commercial RNase III versus authentic *E.coli* RNase III on T7 R1.1 mRNA, defining the HCV cleavages as secondary type (19,21)

While performing the reverse competition experiments described above, we found that commercial RNAse III from Ambion, in the buffer and salt conditions used to cleave HCV RNA, cleaved the T7 R1.1 RNA producing four migrating bands (Figure 5C), instead of two bands as expected from a single primary cleavage event. Because a secondary cleavage site has also been described in T7 R1.1 (22) we wanted to distinguish if, with the Ambion enzyme preparation and in our salt conditions, we were dealing with the reported secondary RNase III cleavage type, on the one hand; or an ssRNase-specific contaminant in the commercial RNase III preparation or peculiar behavior of the commercial RNase III preparation, on the other hand.

A series of experiments were performed to distinguish among these alternatives. We used the T7 R1.1 RNA substrate to characterize (i) the activity of the recombinant enzyme from Ambion, as well as RNase III preparations from two other companies, in buffer conditions of the standard RNase III reaction and in comparison with natural *E.coli* enzyme; (ii) the activity of the Ambion enzyme on R1.1 RNA substrate in the buffer and salt conditions used in this paper, taking also as reference the authentic RNase III preparation; and (iii) the secondary cleavage site of the Ambion enzyme in R1.1.

(i) Enzymes from Ambion, Epicenter, New England Biolabs and the natural *E.coli* RNase III were tested against the R1.1 substrate, transcribed in the presence of [α-^{32}P]GTP. All reactions contained 0.5 µl of RNase III enzymes, a large excess of carrier tRNA, RNA substrate and the 'high salt original RNase III buffer—0.01 M Tris–HCl, pH 7.6, 0.13 M NH_4Cl and 0.01 M $MgCl_2$ (18,25). While natural RNase III enzyme preparations—one from a phosphocellulose column peak (18,21) and another from a DEAE–Sephadex column peak (18,21)—gave two main product bands (corresponding to bands B and E in Figure 6—resulting from primary cleavage of R1.1) and two additional faint bands (corresponding to bands C and D in Figure 6), all three commercial enzymes, including that from Ambion, clearly showed four bands (data not shown). The different pattern was probably due to the fact that the natural RNase III preparations had much lower concentrations than the commercial preparations. This explanation was also supported by the effect of 2 µg of poly(I–C) dsRNA competitive inhibitor on the reactions, which drastically decreased the activity of the natural enzyme preparation while only slightly affecting the reactions of the much more concentrated commercial enzyme preparations (data not shown). Because the four bands appeared with the authentic RNase III purified without protein fusion techniques in reactions carried out under high salt conditions, because they arise in the presence of excess ssRNA and because their production is inhibited by dsRNA competitor, we can use these results to validate the specificity of commercial enzyme with respect to the natural enzyme.

(ii) Several changes were made in the reaction conditions to confirm the hypothesis of specific secondary RNase III cleavage in R1.1 RNA. First, Ambion RNase III was used at dilution 1/10 and 1/100, and was compared with

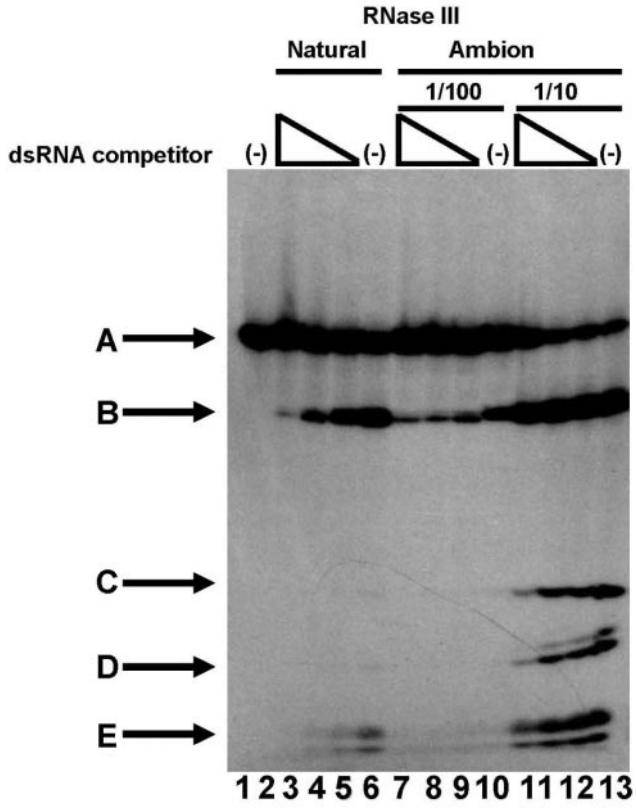

Figure 6. Characterization of commercial RNase III secondary cleaving activity in comparison to the natural enzyme. Activity of the natural and commercial RNase III in buffer under working conditions (lower salt). Lane 1 is the R1.1 substrate incubated in buffer alone—it runs as band A. Lanes 2–4, natural RNase III and R1.1 substrate incubated in the presence of 9, 3 and 1 μg of poly(I–C) dsRNA competitor; lane 5, control reaction with no dsRNA; lanes 6–9 all contain substrate and 1 μl of Ambion RNase III at a 1/100 dilution; lanes 6–8 contain decreasing dsRNA competitor as in lanes 2–4, while lane 9 contains no dsRNA; lanes 10–13 are identical to lanes 6–9, except that they contain 1 μl of 1/10 Ambion RNase III. At the lower enzyme: substrate ratio, bands C and D are only faintly present, and they disappear at once when the dsRNA competitor is added.

the authentic RNase III (DEAE–sephadex column peak); second, increasing amounts of competitor were used; and third, the high salt buffer conditions were replaced by the buffer and salt conditions used in this work, involving lower monovalent salt (Figure 6A, 0.05 M versus 0.13 M). It was observed that at the lower enzyme:substrate ratio, bands C and D are only faintly present, and they disappear at once when the dsRNA competitor is added. Significantly, in lanes 5–2 of Figure 6 this behavior was mimicked by the authentic RNase III enzyme. It is clear that in lane 5, the control reaction with no dsRNA, bands C and D are obviously present; they then disappear as the dsRNA concentration is raised in lanes 4–2. Thus, the reaction was favored by high enzyme:substrate ratios and by lower salt conditions and is effectively inhibited by dsRNA competitors, as expected for a specific secondary cleavage event (21).

(iii) Fingerprint analysis of the secondary cleavage site of R1.1 RNA using the Ambion enzyme was located within the same T1 fragment product as that of the natural enzyme (data not shown).

Cleavage sequences surrounding HCV 5′ and 3′ cleavages reside in a single RNA structural motif with double-stranded character

The two sequences surrounding both cleavage sites in HCV RNA contain a high degree of complementarity. If both cleavage sites participate in a single RNA motif with double-stranded characteristics, deletion of one of the two complementary sequences should also prevent cleavage in the other. We prepared S_3 substrate, which spanned bases 1–402 and lacked the sequence that comprises 3′ the cleavable site (Figure 1). After RNase III incubation, a set of very faint bands migrating closely together and below the S_3 substrate appeared in the gel electrophoresis, but the appearance of these bands is not RNase III dependent as their presence was not affected by incubation with dsRNA. In addition, this 402-base substrate was unable to compete with T7 R.1.1 RNA cleavage by RNase III (data not shown). Thus, S_3 substrate has lost the RNA structure that provides sensitivity to RNase III at the 5′-proximal site.

In a second type experiment, a ribo-oligonucleotide complementary to positions 23–43 (5′-rGGAGUCAUGU-AUGGCGGAGUC-3′), within which the 5′ cleavage site is located, was hybridized in excess concentration (15 nM) to block the hypothetical downstream Watson–Crick binding region in HCV RNA substrates (0.6 nM) containing the 3′ end cleavage site. S_1 substrate was pre-heated in the absence or presence of the ribo-oligonucleotide, buffer added, and the reactions cooled to 37°C, when the RNase III enzyme was added. Aliquots were obtained during the time course of the reaction and run on polyacrylamide gels. In Figure 7, it may be observed that in the presence (+) of the complementary ribo-oligonucleotide the band pattern of the products changed with respect to those incubated without the ribo-oligonucleotide (−). Specifically, a different pattern appeared, consistent with RNase III cleavage directed solely by the ribo-oligonucleotide. This proved that blocking the 5′ sequence motif impedes the formation of the RNA structure required for cleavage at the 3′ end. Together, the two experiments represent direct proof of the interaction between sequences containing both cleavages, enclosing the HCV IRES (Figure 8).

DISCUSSION

Here, we have provided evidence that RNase III from *E.coli* cleaves specifically and with high efficiency at sites within two sequence domains in the HCV IRES, which we have mapped to one region containing bases 27 and 33, and another region containing base 439 (Figures 1–3). The first region is immediately upstream from the HCV IRES domain, while the other is ∼70 bases downstream [assuming that the IRES includes 30 nt of sequence downstream from the AUG start codon (34)]. Furthermore, we have confirmed by end group determination and substrate competition experiments that both natural and commercial RNase III preparations carry out this reaction (Figures 4–6). In addition, we have shown by several criteria that these HCV cleavages by RNase III fall into the category of specific secondary cleavages (Figure 6).

Because cleavage within one RNase III-sensitive region of HCV requires coordinated cleavage within the other (Figure 7), we propose that the two widely separated sequence elements

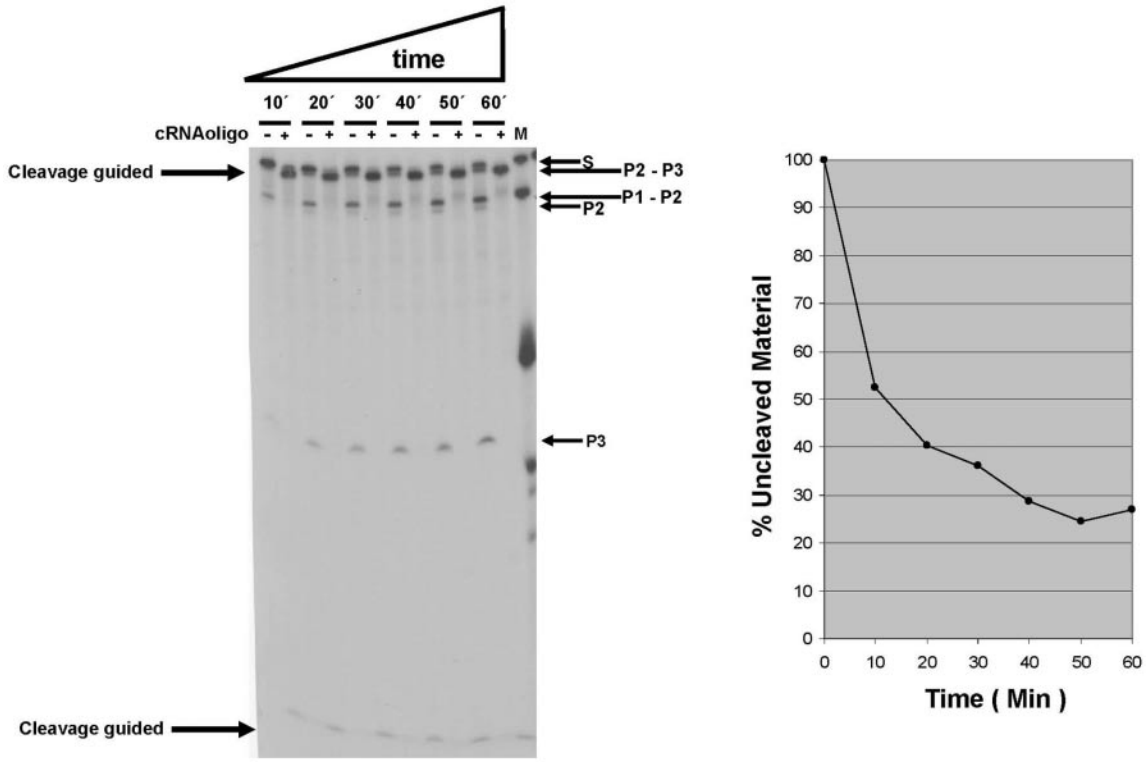

Figure 7. The 5′ and 3′ cleavages in HCV RNA occur in a single structural motif. Kinetic analysis of *E.coli* RNAse III cleavage of HCV RNA in the presence or absence of a complementary RNA oligonucleotide. Left panel: autoradiogram of RNase III cleavage of internally labeled S_1 HCV RNA transcript in the presence (+) or in the absence (−) of a synthetic RNA oligonucleotide complementary to HCV nt 23–43 (5′-GGAGUGAUCUAUGGUGGAGUG-3′). HCV RNA substrate (0.6 nM final concentration) was pre-heated at 90°C for 1 min, before the addition of reaction buffer [10 mM HEPES–KOH, pH 7.5, 10 mM $Mg(OAc)_2$ and 100 mM $NH_4(OAc)$] and left to cool down to room temperature. Cleavage reactions were performed with 20 U RNAsin, and 0.0005 U/μl (final concentration) of *E.coli* RNase III, in the presence of 1 μg/μl of yeast tRNA, and carried out at 37°C in a volume of 10 μl for 1 h. These optimal conditions were used in all of the experiments. In (+) reactions the synthetic complementary RNA oligonucleotide was added to a final concentration of 15 nM. Lane 13 ('M') contains RNA molecular weight markers composed of transcripts with a length of 82, 99, 110, 400 and 570 (S_1) nt. Lanes starting from the left represent sequentially 10, 20, 30, 40, 50 and 60 min of incubation with RNase III without (−) or with (+) complementary RNA oligonucleotide. Cleavage products were separated on 4% denaturing polyacrylamide gels and visualized by autoradiography. The arrows on the left indicate the products of the RNase III cleavage directed by the complementary oligonucleotide and on the right; the products of RNase III alone (P1+P2, P2 and P3) are indicated. Quantitation was performed with a Radioisotopic Image Analyzer. Right panel: Graphic representation of the time course processing of S_1 by *E.coli* RNAse III in the absence of the complementary RNA oligonucleotide.

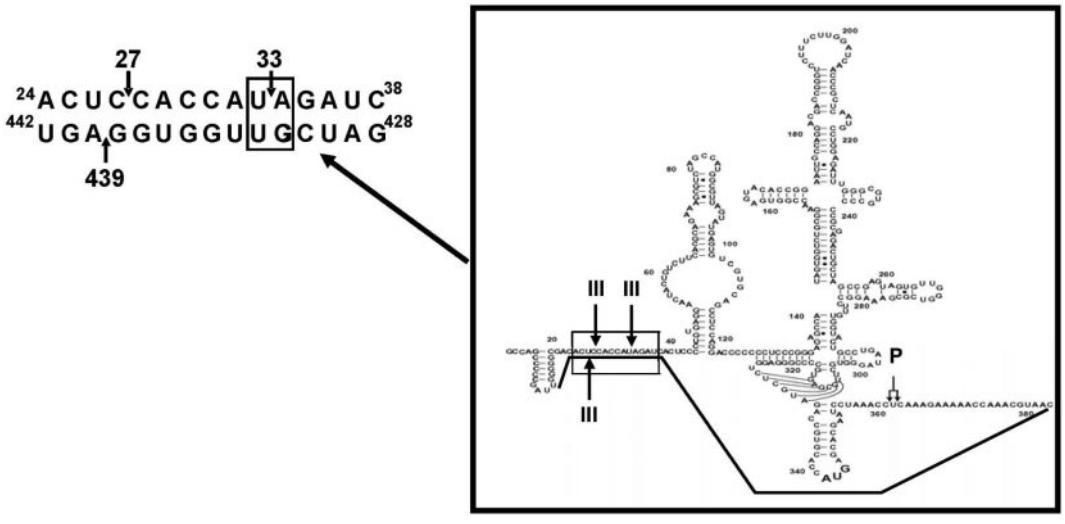

Figure 8. Diagram including the proposed structural motif which contains both RNase III cleavage domains and encloses the HCV IRES. On the left is shown the interaction between nt 24 and 38 of the 5′ (UTR) with the nt 428–442 of the HCV Core–coding sequence. The arrows represent the RNase III cleavage sites. The 'loop' is shown within a box on the right of the figure. Symbol 'P' refers to the cleavage position of human RNase P, which is another RNA structure dependent nuclease. After the annealing, both RNase III and RNase P cleavage sites became in close proximity.

which comprise them in fact form a base-paired structure (Figure 8), which is present at sufficient frequency to allow over 80% of the substrate to undergo RNase III cleavage (Figure 7). This conclusion is supported by the fact that 5′-proximal RNase III cleavage fails to occur in the absence of the 3′-proximal sequence (data not shown), and 3′ cleavage is blocked when the 5′ cleavable region is hybridized to a complementary RNA oligonucleotide (Figure 7). We will briefly address how these findings relate to other RNase III-specific reactions; how the structured element identified here relates to previously identified HCV IRES structures and how a dsRNA structure bracketing the IRES might affect HCV gene expression.

E.coli RNase III carries out three principal reactions (19): the digestion of perfect dsRNA to 15 bp fragments, independent of sequence; primary cleavage, usually of imperfectly base-paired regions which have evolved to play a role in host rRNA processing; and secondary cleavage, in which imperfectly base-paired regions from other RNAs, which resemble primary RNase III sites, are cleaved. While both dsRNA digestion and primary cleavage by RNase III are optimized in higher (>0.1 M monovalent cation) salt and lower enzyme:substrate conditions, secondary cleavage is favored at lower salt and higher enzyme:substrate ratios.

Cleavage sites sensitive to RNase III under low salt conditions, such as the ones described here in HCV RNA, have been reported in earlier studies on RNase III. In particular, RNase III cleavage of the genomic RNAs of several eukaryotic RNA viruses, including poliovirus (35), adenovirus (36) and vesicular stomatitis virus (37,38), as well as mammalian rRNA (36), have been reported. However, these earlier findings neither did lead to a general explanation for the presence of such RNase III sites, nor did they give rise to further research, in contrast to the situation with prokaryotic RNase III sites. This lack of follow-up probably took place because mammalian RNase III-like enzymes had not yet been discovered; and because the earlier eukaryotic RNase III signals were not mapped to the base their exact RNA structure could not be ascertained.

Previously identified RNA structural elements in the HCV IRES include a pseudoknot just upstream from the AUG initiator codon (1–4), a UV-crosslinkable tertiary element in stem–loop II (39), two E-loop structures (40), one in the upper part of stem–loop II and the other in stem–loop IIId, a domain which undergoes UV-activated self-cleavage near the top of stem–loop II (A. J. Lyons and H. D. Robertson, manuscript submitted) and a tRNA-like element near the AUG start codon recognized by human RNase P (26,41). While functions have been suggested for some of these elements (1,26,41) others still await assignment. The presence of such elements in the near vicinity of a structural domain capable of undergoing RNase III cleavage requires further consideration.

First, there are a growing number of similarities between the HCV IRES and the adjacent core protein coding sequence, especially the first 1/3 thereof. Our data show that an RNAse III-sensitive structure converts the 5′-UTR and 1/3 of the core-coding region into a circular RNA loop, closed by base pairing as shown in Figure 8. The IRES and core-coding regions, in addition to sharing a highly structured character (15,42,43), overlap in several other ways. First, the IRES contains the first 30 bases of the core-coding sequence. Second, sequences required for HCV IRES cleavage by human RNase P may include bases at or near the IRES/core-coding junction (26,41,44). In addition, the IRES and core-coding regions share a low degree of sequence variation (1,45,46). Together, these findings suggest that the two domains in this part of the HCV genome may have a structural and evolutionary unity, despite the coding/non-coding discontinuity, an idea which is strengthened by our finding that each domain contributes one of the two required elements which form the RNase III-sensitive structure whose discovery we report here.

The circular RNA of the hepatitis delta virus (HDV) is also an RNA circle (closed covalently rather by hydrogen bonds) which contains highly structured non-coding and coding regions that are adjacent to each other (47). Furthermore, the ‘delta antigen’ protein, encoded by HDV RNA, is a nucleic acid binding protein like the HCV core protein (48). Both HDV and the HCV IRES region also contain a motif highly sensitive to UV irradiation in their non-coding regions (39,49). Both HCV and HDV also infect the liver to provoke consistent infections (1,48) and could reflect the evolution of a common unit of RNA expression pathogenic to the human liver.

The HCV RNase III signal maps within 79 and 130 bases of a previously described RNase P signal (44). With regard to the presence of tRNA-like structure which stimulates RNase P cleavage in the near vicinity of RNase III cleavage sites, there are several noteworthy examples where these two kinds of signals appear close together, including the *E.coli* rRNA precursor molecule, the 10sa RNA molecule, and the mRNA of several bacteriophages (36,50–53) and in structural RNAs in yeast (54). The significance to *in vivo* function of both of these signal types remains to be established for HCV, although in the other cases mentioned both types participate in a common RNA processing pathway.

The presence of a structural element flanking the HCV IRES raises questions about how it may affect IRES activity. The most direct role would be in regulating the access of ribosomes to the IRES start signal. In their study of phylogenetic and mutational data favoring some type of interaction between HCV bases 24–38 and 428–442, Kim *et al*. (16) suggested that such an element might inhibit translation. Further studies will be required to measure the ability of IRES-specific components (initiation factors, ribosomal subunits, RNase P) to bind HCV RNA with versus without the RNase III-sensitive structure. It is interesting to note, in this regard, that the vast majority of studies on translation stimulated by the HCV IRES, both *in vitro* and in cells and using either mono- or di-cistronic constructs, have used HCV IRES sequences spanning only bases 1–400, lacking the RNase III-sensitive structure. Several studies on ribosome binding and translation of an HCV mRNA spanning bases 1–1350 (which contains the RNase III-sensitive structure) are available (55,56), but a systematic comparison of protein synthesis stimulated by the same HCV mRNA molecule, with and without the RNase III-sensitive structure (which can be blocked by cleavage or by oligonucleotides, as shown in Figure 7B), is yet to be performed. Such studies will be necessary to determine whether the RNase III-sensitive structure promotes or inhibits ribosome binding and translation, or has no effect.

The 5′-UTR of HCV genomic RNA encodes the start signal for genomic strand RNA synthesis (which is the 3′ end of the antigenomic, or minus, strand), as well as the IRES itself,

suggesting a role for some of these sequences in both processes. One of the difficulties concerning a structure containing the two domains studied here—one near the 5′ end of the HCV UTR involving bases 24–38, the other including bases 428–442—was that earlier work had suggested a structure called stem–loop VI within the core-coding domain (15,43), in which bases 428–442 are base paired with bases 495–508. In fact, the ability of these two potential structures to alternate could regulate a particular HCV RNA molecule's ability to participate in translation versus replication. Experiments comparing the stability of the proposed stem–loop VI to the RNase III-sensitive structural element studied here will need to be performed before this idea can be evaluated.

The conditions described here allow reproducible, structure-dependent cleavage reactions which can produce specific RNA fragments for a variety of assays. For example, binding of translation initiation factors, La protein, PKR and ribosomal proteins could be conducted before and after RNase III treatment. In this way, both the boundaries of the IRES domain, and its structural inter-dependence with the flanking, RNase III-sensitive sequences, can be ascertained. Whatever the role of the RNase-sensitive structure, it allows new basic studies on IRES structure and function, and provides opportunities for RNAi and ribozyme therapeutics as well.

ACKNOWLEDGEMENTS

The authors thank Tsering Choden and Drs Maria Piron, Anna Nadal, Rosario Sabariegos, Isabel Leal and Javier Martinez for their enthusiastic scientific support. Plasmidic vector pN (1–4728) Bluescript was kindly provided by M. Honda and S. M. Lemon, and plasmid DNA template for RNA R1.1 transcripts was supplied by Dr A. Nicholson. This work was supported by a grant from the US NIH and by a Johnson & Johnson Focused Giving award to H.D.R., and by Ministerio de Ciencia y Tecnologia Grant BIO-04-06114 and foundation FIPSE, grant number 36293/02 to J.G. Funding to pay the Open Access publication charges for this article was provided by Ministerio de Ciencia Tecnologia Grant BIO-04-06114.

Conflict of interest statement. None declared.

NOTE ADDED IN PROOF

Dr Hugh D. Robertson, our friend and co-author of this paper died August 22, 2005.

REFERENCES

1. Houghton,M. (1996) Hepatitis C virus. In Fields,B.N., Knipe,D.N. and Howley,P.N. (eds), *Field's Virology*. Lippincott-Raven, Philadelphia, PA, pp. 1035–1057.
2. Tsukiyama-Kohara,K., Iizuka,N., Kohara,M. and Nomoto,A. (1992) Internal ribosome entry site within hepatitis C virus RNA. *J. Virol.*, **66**, 1476–1483.
3. Brown,E.A., Zajac,A.J. and Lemon,S.M. (1994) *In vitro* characterization of an internal ribosomal entry site (IRES) present within the 5′ nontranslated region of hepatitis A virus RNA: comparison with the IRES of encephalomyocarditis virus. *J. Virol.*, **68**, 1066–1074.
4. Wang,C., Sarnow,P. and Siddiqui,A. (1994) A conserved helical element is essential for internal initiation of translation of hepatitis C virus RNA. *J. Virol.*, **68**, 7301–7307.
5. Luo,G., Xin,S. and Cai,Z. (2003) Role of the 5′-proximal stem–loop structure of the 5′ untranslated region in the replication and translation of hepatitis C virus RNA. *J. Virol.*, **77**, 3312–3318.
6. Lohmann,V., Korner,F., Koch,J., Herian,U., Theilmann,L. and Bartenschlager,R. (1999) Replication of subgenomic hepatitis C virus RNAs in a hepatoma cell line [see comments]. *Science*, **285**, 110–113.
7. Blight,K.J., Kolykhalov,A.A. and Rice,C.M. (2000) Efficient initiation of HCV RNA replication in cell culture. *Science*, **290**, 1972–1974.
8. Honda,M., Brown,E.A. and Lemon,S.M. (1996) Stability of a stem–loop involving the initiator AUG controls the efficiency of internal initiation of translation on hepatitis C virus RNA. *RNA*, **2**, 955–968.
9. Honda,M., Ping,L.H., Rijnbrand,R.C., Amphlett,E., Clarke,B., Rowlands,D. and Lemon,S.M. (1996) Structural requirements for initiation of translation by internal ribosome entry within genome-length hepatitis C virus RNA. *Virology*, **222**, 31–42.
10. Odreman-Macchioli,F., Baratlle,F.E. and Buratti,E. (2001) Mutational analysis of the different bulge regions of hepatitis C virus domain II and their influence on internal ribosome entry site translational activity. *J. Biol. Chem.*, **276**, 41648–41655.
11. Reynolds,J.E., Kaminski,A., Carroll,A.R., Clarke,B.E., Rowlands,D.J. and Jackson,R.J. (1996) Internal initiation of translation of hepatitis C virus RNA: the ribosome entry site is at the authentic initiation codon. *RNA*, **2**, 867–878.
12. Bukh,J., Purcell,R.H. and Miller,R.H. (1992) Sequence analysis of the 5′ non-coding region of hepatitis C virus. *Proc. Natl Acad. Sci. USA*, **89**, 4942–4946.
13. Smith,D.B., Mellor,J., Jarvis,L.M., Davidson,F., Kolberg,J., Urdea,M., Yap,P.L. and Simmonds,P. (1995) Variation of the hepatitis C virus 5′ non-coding region: implications for secondary structure, virus detection and typing. The International HCV Collaborative Study Group. *J. Gen. Virol.*, **76**, 1749–1761.
14. Saiz,J.C., Lopez de Quinto,S., Ibarrola,N., López-Labrador,F.X., Sánchez-Tapias,J.M., Rodés,J. and Martínez-Salas,E. (1999) Internal initiation of translation efficiency in different hepatitis C genotypes isolated from interferon treated patients. *Arch. Virol.*, **144**, 215–229.
15. Honda,M., Rijnbrand,R., Abell,G., Kim,D. and Lemon,S. (1999) Natural variation in translational activities of the 5′ nontranslated RNAs of hepatitis C virus genotypes 1a and 1b: evidence for a long-range RNA–RNA interaction outside of the internal ribosomal entry site. *J. Virol.*, **73**, 4941–4951.
16. Kim,Y.K., Lee,S.H., Kim,C.S., Seol,S.K. and Jang,S.K. (2003) Long-range RNA–RNA interaction between the 5′ nontranslated region and the core-coding sequences of hepatitis C virus modulates the IRES-dependent translation. *RNA*, **9**, 599–606.
17. Robertson,H.D., Webster,R.E. and Zinder,N.D. (1967) A nuclease specific for double-stranded RNA. *Virology*, **12**, 718–719.
18. Robertson,H.D., Webster,R.E. and Zinder,N.D. (1968) Purification and properties of ribonuclease III from *Escherichia coli*. *J. Biol. Chem.*, **243**, 82–91.
19. Robertson,H.D. (1982) *Escherichia coli* ribonuclease III cleavage sites. *Cell*, **30**, 669–672.
20. Nicholson,A.W. (2003) The ribonuclease III superfamily: forms and functions in RNA maturation, decay, and gene silencing. In Hannon,G.J. (ed.), *RNAi Guide to Gene Silencing*. Cold Spring Harbor Laboratory Press, Chapter 8, pp. 149–174.
21. Dunn,J.J. (1976) RNase III cleavage of single-stranded RNA. Effect of ionic strength on the fidelity of cleavage. *J. Biol. Chem.*, **251**, 3807–3814.
22. Li,H.L., Chelladurai,B.S., Zhang,K. and Nicholson,A.W. (1993) Ribonuclease III cleavage of a bacteriophage T7 processing signal. Divalent cation specificity, and specific anion effects. *Nucleic Acids Res.*, **21**, 1919–1925.
23. Robertson,H.D., Dickson,E. and Dunn,J.J. (1977) A nucleotide sequence from a ribonuclease III processing site in bacteriophage T7 RNA. *Proc. Natl Acad. Sci. USA*, **74**, 822–826.
24. Dunn,J.J. and Studier,F.W. (1983) Complete nucleotide sequence of bacteriophage T7 DNA and the locations of T7 genetic elements. *J. Mol. Biol.*, **166**, 477–535.
25. Robertson,H.D. (1990) *Escherichia coli* Ribonuclease III. *Methods Enzymol.*, **181**, 189–202.
26. Nadal,A., Martell,M., Lytle,J.R., Lyons,A.J., Robertson,H.D., Cabot,B., Esteban,J.I., Esteban,R., Guardia,J. and Gomez,J. (2002) Specific cleavage of hepatitis C virus RNA genome by human RNase P. *J. Biol. Chem.*, **277**, 30606–30613.

27. Hansen,A., Pfeiffer,T., Zuleeg,T., Limmer,S., Ciesiolka,J., Feltens,R. and Hartmann,R.K. (2001) Exploring the minimal substrate requirements for *trans*-cleavage by RNase P holoenzymes from *Escherichia coli* and *Bacillus subtilis*. *Mol. Microbiol.*, **41**, 131–143.
28. Branch,A.D., Benenfeld,B.J. and Robertson,H.D. (1989) RNA fingerprinting. *Methods Enzymol.*, **180**, 130–154.
29. King,T.C., Sirdeshmukh,R. and Schlessinger,D. (1984) RNase III cleavage is obligate for maturation but not for function of *Escherichia coli* pre-23S rRNA. *Proc. Natl Acad. Sci. USA*, **81**, 185–188.
30. Paddock,G.V., Fukada,K., Abelson,J. and Robertson,H.D. (1976) Cleavage of T4 species I ribonucleic acid by *Escherichia coli* ribonuclease III. *Nucleic Acids Res.*, **3**, 1351–1371.
31. Robertson,H.D. and Dunn,J.J. (1975) Ribonucleic acid processing activity of *Escherichia coli* ribonuclease III. *J. Biol. Chem.*, **250**, 3050–3056.
32. Adams,R.L.P., Knowler,J.T. and Leader,D.P. (1992) Degradation of nucleic acids. In Adews,R.L.P., Knowler,J.T. and Leader,D.P. (eds). *The Biochemistry of the Nucleic Acids*. Chapman and Hall Ltd, London, pp. 97–133.
33. Robertson,H.D., Altman,S. and Smith,J.D. (1972) Purification and properties of a specific *Escherichia coli* ribonuclease which cleaves a tyrosine transfer ribonucleic acid precursor. *J. Biol. Chem.*, **247**, 5243–5251.
34. Fletcher,S.R., Ali,I.K., Kaminski,A., Digard,P. and Jackson,R.J. (2002) The influence of viral coding sequences on pestivirus IRES activity reveals further parallels with translation initiation in prokaryotes. *RNA*, **8**, 1558–1571.
35. Harris,T.J., Dunn,J.J. and Wimmer,E. (1978) Identification of specific fragments containing the 5′ end of poliovirus RNA after ribonuclease III digestion. *Nucleic Acids Res.*, **5**, 4039–4054.
36. Westphal,H. and Crouch,R.J. (1975) Cleavage of adenovirus messenger RNA and of 28S and 18S ribosomal RNA by RNase III. *Proc. Natl Acad. Sci. USA*, **72**, 3077–3081.
37. Wertz,G.W. and Davis,N.L. (1979) RNase III cleaves vesicular stomatitis virus genome-length RNAs but fails to cleave viral mRNA's. *J. Virol.*, **30**, 108–115.
38. Wertz,G.W. and Davis,N. (1981) Characterization and mapping of RNase III cleavage sites in VSV genome RNA. *Nucleic Acids Res.*, **9**, 6487–6503.
39. Lyons,A.J., Lytle,J.R., Gómez,J. and Robertson,H.D. (2001) Hepatitis C virus internal ribosome entry site RNA contains a tertiary structural element in a functional domain of stem–loop II. *Nucleic Acids Res.*, **29**, 2535–2541.
40. Lukavsky,P.J., Kim,I., Otto,G.A. and Puglisi,J.D. (2003) Structure of HCV IRES domain II determined by NMR. *Nature Struct. Biol.*, **10**, 1033–1038.
41. Lyons,A.J. and Robertson,H.D. (2003) Detection of tRNA-like structure through RNase P cleavage of viral internal ribosome entry site RNAs near the AUG start triplet. *J. Biol. Chem.*, **278**, 26844–26850.
42. Martell,M., Briones,C., de Vicente,A., Piron,M., Esteban,J.I., Esteban,R., Guardia,J. and Gomez,J. (2004) Structural analysis of hepatitis C RNA genome using DNA microarrays. *Nucleic Acids Res.*, **32**, e90.
43. Walewski,J.L., Gutierrez,J.A., Branch-Elliman,W., Stump,D.D., Keller,T.R., Rodriguez,A., Benson,G. and Branch,A.D. (2002) Mutation Master: profiles of substitutions in hepatitis C virus RNA of the core, alternate reading frame, and NS2 coding regions. *RNA*, **8**, 557–571.
44. Piron,M., Beguiristain,N., Nadal,A., Martinez-Salas,E. and Gomez,J. (2005) Characterizing the function and structural organization of the 5′ tRNA-like motif within the hepatitis C virus quasispecies. *Nucleic Acids Res.*, **33**, 1487–1502.
45. Bukh,J., Purcell,R.H. and Miller,R.H. (1992) Sequence analysis of the 5′ noncoding region of hepatitis C virus. *Proc. Natl Acad. Sci. USA*, **89**, 4942–4946.
46. Bukh,J., Purcell,R.H. and Miller,R.H. (1994) Sequence analysis of the core gene of 14 hepatitis C virus genotypes. *Proc. Natl Acad. Sci. USA*, **91**, 8239–8243.
47. Robertson,H.D. (1996) How did replicating and coding RNAs first get together? *Science*, **274**, 66–67.
48. Lai,M.C. (1999) Hepatitis delta virus. In Grouoff,A. and Webster,R.G. (eds). *Encyclopedia of Virology*. Academic Press, London, UK, Vol. 1, pp. 644–669.
49. Branch,A.D., Benenfeld,B.J., Baroudy,B.M., Wells,F.V., Gerin,J.L. and Robertson,H.D. (1989) An ultraviolet-sensitive RNA structural element in a viroid-like domain of the hepatitis delta virus. *Science*, **243**, 649–652.
50. Makarov,E.M. and Apirion,D. (1992) 10Sa RNA: processing by and inhibition of RNase III. *Biochem. Int.*, **26**, 1115–1124.
51. Frank,D.N. and Pace,N.R. (1998) Ribonuclease P: unity and diversity in a tRNA processing ribozyme. *Annu. Rev. Biochem.*, **67**, 153–180.
52. Dunn,J.J. and Studier,F.W. (1973) T7 early RNAs are generated by site-specific cleavages. *Proc. Natl Acad. Sci. USA*, **70**, 1559–1563.
53. Dunn,J.J. and Studier,F.W. (1973) T7 early RNAs and *Escherichia coli* ribosomal RNAs are cut from large precursor RNAs *in vivo* by ribonuclease 3. *Proc. Natl Acad. Sci. USA*, **70**, 3296–3300.
54. Tollervey,D. (1997) RNA Processing. *EMBL Research Reports,* pp. 134–136.
55. Lytle,J.R., Wu,L. and Robertson,H.D. (2001) The ribosome binding site of hepatitis C virus mRNA. *J. Virol.*, **75**, 7629–7636.
56. Lytle,J.R., Wu,L. and Robertson,H.D. (2002) Domains on the hepatitis C virus internal ribosome entry site for 40s subunit binding. *RNA*, **8**, 1045–1055.